

FINITE ELEMENT ANALYSIS OF TENSION-WEAK MATERIALS

By

Frank E. Weisgerber¹, M., ASCE

and

Mohammad Rezaiee-Pajand²

INTRODUCTION

Many common engineering materials are significantly weaker in tension than in compression. Concrete, rock, soil, coal and ice are obvious examples. Although analyses for stress and displacements of systems composed of these materials are frequently desired in engineering practice, currently only two approaches to the multi-axial finite element analysis of tension-weak material systems are generally seen: linear elastic analyses from which one may confidently extrapolate qualitative information at best; and considerably more complex analyses within large-scale research programs (largely academic). As the latter approach eventually leads to information useful to engineering practice, it needs to be encouraged and expanded. However, such an approach appears to be impracticable in the ordinary design office. To use analysis of concrete systems as an example, Gerstle [1] points out that "in spite of the general recognition of the non-linear character of concrete response to compressive stress states, most [recent] analyses use a purely elastic description of the concrete behavior up to the point of cracking or crushing."

Precise analysis of systems composed of tension-weak materials is made difficult by several factors related to material properties and behavior. Most of these materials tend to have highly variable elastic properties so that an analysis must be based either on approximate average values or be preceded by extensive testing to obtain values more suited to the particular case at hand. In some cases, the assumption of isotropy and homogeneity may be suspect. Additionally, the low tensile strength of these materials causes non-linear response even to relatively low load levels. This response is not well approximated by linear elastic analysis. Attempts at non-linear analyses generally require the definition of yield and failure criteria for the materials and here again one must either adopt average values or perform even more extensive testing. Not only does one need to determine parameter magnitudes, but also the very form of the yield and/or failure surfaces since there appears to be no general agreement on these for most non-metallic materials.

1. Assistant Professor, University of Cincinnati, Cincinnati, Ohio.
2. Graduate Student, University of Pittsburgh, Pittsburgh, Pennsylvania.

The gap between the two current approaches (the assumption of linear elastic response and the complex non-linear formulation) is large with respect to both accuracy of results and practicability. This paper describes an attempt to partially fill that gap by developing and illustrating a manner of analysis which, while still producing approximate results, does account for the non-linear characteristics of the material and which can be expected to yield useful data economically. In particular, this paper describes the application of elasto-plastic finite element analysis to tension-weak material using a linearized yield surface in an incremental technique.

Since the basic formulation and solution method follow rather standard procedure, which is fully described in previous literature, these are only summarized in the following sections. Incremental and matrix notation are used here without formal justification. Development of particulars extends only to the case of plane stress. Additional development is currently in progress for the plane strain and fully three-dimensional cases.

FUNDAMENTALS

In order to model the post-yield response of a material, it is necessary to establish three fundamental items in addition to the elastic properties: an initial yield condition, defining the elastic limit of the material; a flow rule, relating inelastic strain to the stresses; and a hardening rule, defining the condition for continuing or subsequent yield. Failure criteria, distinct from yield criteria, may also be established. Furthermore, it is commonly necessary to assume that small increments of strain may be separated into elastic and plastic components. That is,

$$\delta \epsilon = \delta \epsilon^e + \delta \epsilon^p \quad (1)$$

Yield Condition. A yield condition may generally be expressed by a yield function, F , written in terms of a stress state, σ_{ij} , and a hardening parameter, κ , as

$$F = f(\sigma_{ij}, \kappa) \quad (2)$$

In evaluation of a particular stress state in relation to the yield function, $F < 0$ represents an elastic state, $F = 0$ represents a plastic state, and $F > 0$ is an inadmissible stress state. The yield condition is discussed in detail in a subsequent section of this paper.

Flow Rule. The flow rule commonly used in elasto-plastic analysis is based on Drucker's Postulate and may be written in incremental form as

$$\delta \epsilon_{ij}^P = \lambda \frac{\partial F}{\partial \sigma_{ij}} \quad (3)$$

in which $\delta \epsilon_{ij}^P$ is the vector of the plastic components of incremental strains, λ is a scalar of proportionality and σ_{ij} is the vector of total stresses.

Hardening Rule. The choice of the hardening rule used in an analysis depends upon its ability to represent the phenomenon to be studied, its mathematical consistency with the yield function and the ease with which it can be applied within the chosen method of analysis. The precise form of the variation in the yield surface with respect to continued yield is a subject of considerable controversy but one of two basic types of hardening rules are employed in most elasto-plastic analyses: isotropic hardening, which assumes the yield surface expands uniformly in all directions with increasing plastic flow; and kinematic hardening, which assumes a translating yield surface. Combinations and modifications of these two are also used.

In many cases where only monotonically increasing loads are applied to a system, the material may be assumed to harden isotropically and the expansion of the yield surface may be related to a function, $\bar{\sigma}(\eta)$, which may be considered a measure of the "size" of the yield surface. The hardening parameter, η , is conveniently taken as the plastic work density,

$$\eta = \int \sigma_{ij} d\epsilon_{ij}^P \quad (4)$$

but alternate forms are also possible. Initial yield occurs at $\eta = 0$ since prior to yield, no plastic strain exists. The corresponding initial yield stress is denoted by σ_0 , i.e., $\bar{\sigma}(0) = \sigma_0$.

The slope of the $\bar{\sigma}(\eta)$ versus ϵ^P curve is denoted in this paper by H' . This slope is zero for a perfectly plastic material. A positive H' indicates strain-hardening and a negative H' indicates strain-softening.

THE LINEARIZED YIELD SURFACE

The yield surface for a hypothetical tension-weak material is shown in Fig. 1. This form is similar to that often given for concrete. Since it is difficult to find a single function to define the entire surface, a series of functions, each representing a particular region of the surface, is indicated.

Precise definition of a yield condition for a real tension-weak material is difficult to achieve. These are materials with complex behavior. Considerable experimentation has been performed but general agreement has been

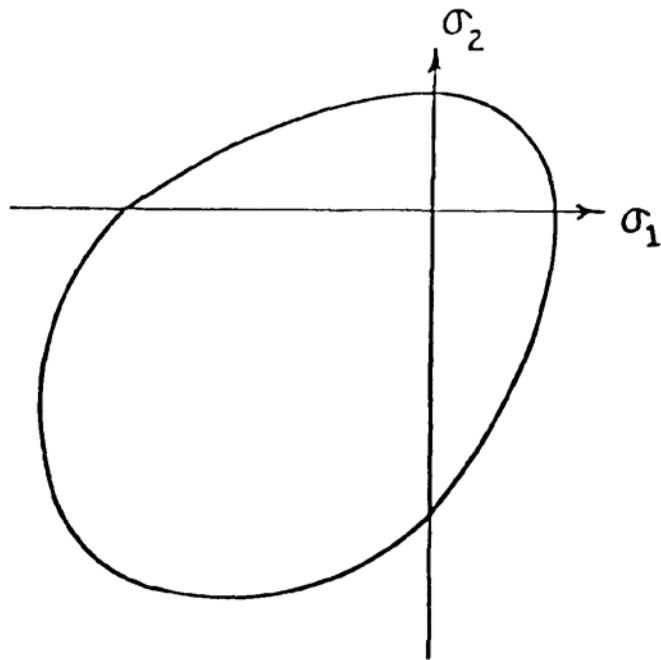


Figure 1. Yield Surface For Hypothetical Tension-Weak Material

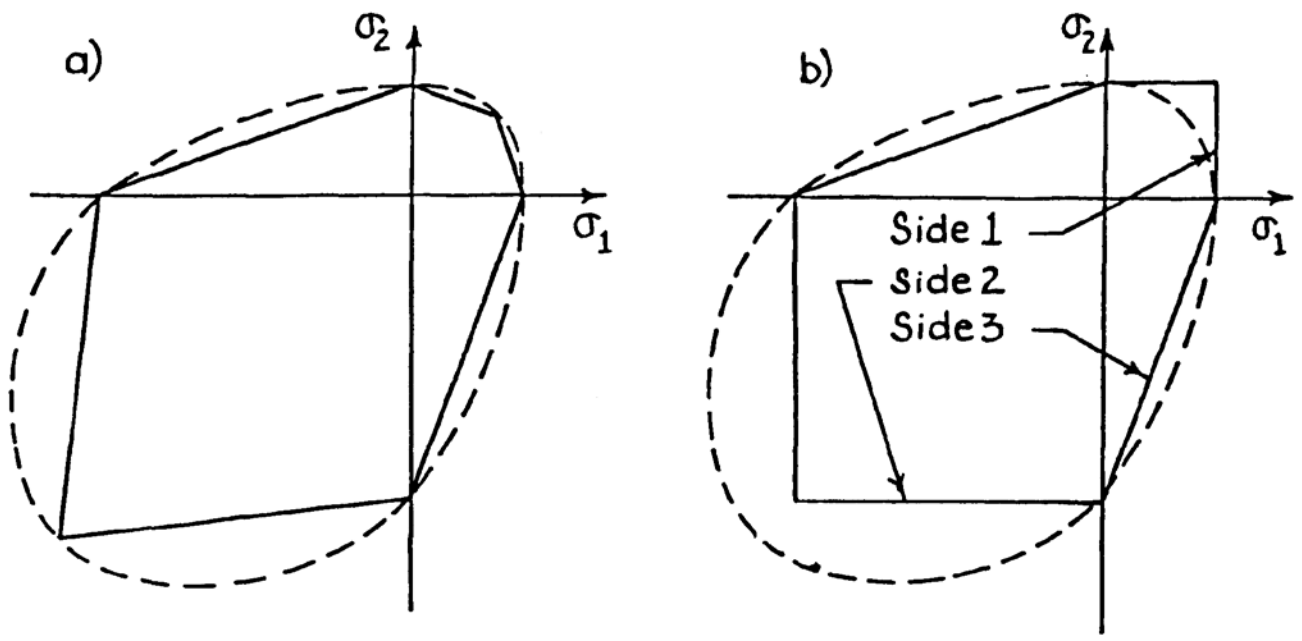


Figure 2. Example Linearized Yield Surfaces

reached on neither the form of the real yield surface nor on the parameter magnitudes. Test results are very sensitive to what would initially seem to be minor variations in experimental procedure. To use concrete as an example, many forms of constitutive relationships have been observed in the literature [2, 3, 4].

Considering that experimentation has shown that the strength, Young's Modulus, and other properties of a tension-weak material may vary widely from sample to sample, the need to find exact representation of the yield function to achieve meaningful solutions to practical engineering design problems becomes doubtful. Accuracy in theoretical form may easily be overshadowed by inaccuracies in parameter magnitudes. Thus, it is not unreasonable to propose the use, for limited cases, of a linearized yield surface that obviously only approximates the actual form. Two such linearized yield surface approximations are shown in Fig. 2. Note also that additional accuracy in form, if desired, could be achieved by use of a few more line segments.

Experimental evidence does indicate that yield surfaces for real materials tend to be curvilinear and thus a linearized yield surface can indeed only be an approximation. However, this approximation has some noteworthy attributes. If the linearized yield surface is inscribed within the assumed correct curvilinear form, it tends to be conservative in that it underestimates initial yield, collapse load and shakedown load while it overestimates post-yield displacements. Furthermore, of the possible yield surfaces which are possible to construct from a limited set of discrete data points, the linearized yield surface is the only one guaranteed, by the normality principle, to exclude all inadmissible stress states.

The use of a linearized yield surface is the exception rather than the rule. However, its previous use has been described in the literature although not with respect to tension-weak material. It is obvious that constructing a yield surface of straight lines must result in corners which represent singularities: points at which the normal vector is not uniquely defined. Unless this direction is itself the objective of the analysis, no practical difficulties arise in the solution procedure. Certainly special constitutive relations associated with the singular points must be derived, but their existence does not compromise the analysis technique.

The special case of a plane stress linearized yield surface as shown in Figure 2b is considered in the remainder of this paper. Letting α denote the ratio of the compressive yield to the tensile yield, this yield surface may be represented by a series of six linear functions written in terms of principal stresses as

$$\begin{aligned}
 F^1 &= \sigma_1 - \bar{\sigma}(k) = 0 \\
 F^2 &= -\sigma_2 - \alpha\bar{\sigma}(k) = 0 \\
 F^3 &= \alpha\sigma_1 - \sigma_2 - \alpha\bar{\sigma}(k) = 0 \\
 F^4 &= \sigma_2 - \bar{\sigma}(k) = 0 \\
 F^5 &= -\sigma_1 - \alpha\bar{\sigma}(k) = 0 \\
 F^6 &= -\alpha\sigma_1 + \sigma_2 - \alpha\bar{\sigma}(k) = 0
 \end{aligned} \tag{5}$$

By invoking the relationship between principal stresses and Cartesian stresses,

$$\begin{aligned}\sigma_1 &= \sigma_x \cos^2 \Theta + \sigma_y \sin^2 \Theta + 2\sigma_{xy} \sin \Theta \cos \Theta \\ \sigma_2 &= \sigma_x \sin^2 \Theta + \sigma_y \cos^2 \Theta - 2\sigma_{xy} \sin \Theta \cos \Theta\end{aligned}\quad (6)$$

in which Θ is the angle between the x-axis and the direction of the major principal stress, these yield functions may be written as follows:

$$\begin{aligned}F^1 &= c^2 \sigma_x + s^2 \sigma_y + 2cs \sigma_{xy} - \bar{\sigma}(\eta) = 0 \\ F^2 &= s^2 \sigma_x - c^2 \sigma_y + 2cs \sigma_{xy} - \alpha \bar{\sigma}(\eta) = 0 \\ F^3 &= (\alpha c^2 - s^2) \sigma_x + (\alpha s^2 - c^2) \sigma_y + 2cs(1 + \alpha) \sigma_{xy} - \alpha \bar{\sigma}(\eta) = 0 \\ F^4 &= s^2 \sigma_x + c^2 \sigma_y - 2cs \sigma_{xy} - \bar{\sigma}(\eta) = 0 \\ F^5 &= -c^2 \sigma_x - s^2 \sigma_y - 2cs \sigma_{xy} - \alpha \bar{\sigma}(\eta) = 0 \\ F^6 &= (\alpha s^2 - c^2) \sigma_x + (\alpha c^2 - s^2) \sigma_y - 2cs(1 + \alpha) \sigma_{xy} - \alpha \bar{\sigma}(\eta) = 0\end{aligned}\quad (7)$$

where $c = \cos \Theta$ and $s = \sin \Theta$.

SOLUTION METHOD

The use of a linearized yield surface is not restricted to a specific technique of non-linear finite element analysis. However, the following discussion does assume that one of the incremental methods is used and the numerical examples were solved using the initial stress method. Because sufficient discussion of the initial stress method already exists in the literature [5], it will not be repeated here. Description of this method as it applies to a linearized yield surface was presented by Weisgerber and Anand [6].

DERIVATION OF THE ELASTO-PLASTIC MATRIX

In an incremental method it becomes necessary to derive the incremental form of the constitutive relationship for material in the yielded state. Thus increments of stress are related to increments of strain as

$$\delta \sigma_{ij} = \underline{D}_{ep} \delta \epsilon_{ij} \quad (8)$$

in which \underline{D}_{ep} is the elasto-plastic stress-strain transformation matrix. For the linearized yield surface, a separate elasto-plastic matrix, \underline{D}_{ep}^i , is required for each function, F^i , in the series defining the yield criterion. An elasto-plastic matrix is required for each corner as well.

In the elastic range, the incremental stress-strain relationship is

$$\delta\sigma_{ij} = \underline{D}_e \delta\varepsilon_{ij}^e \quad (9)$$

where \underline{D}_e is the elastic matrix. The increments of elastic strain are thus

$$\delta\varepsilon_{ij}^e = \underline{D}_e^{-1} \delta\sigma_{ij} \quad (10)$$

Substituting Eqns. 10 and 3 into Eqn. 1 yields an expression for the incremental strain components in material in the yielded state:

$$\delta\varepsilon_{ij} = \underline{D}_e^{-1} \delta\sigma_{ij} + \lambda^i \frac{\partial F^i}{\partial \sigma_{ij}} \quad (11)$$

where the superscript "i" indexes a particular function in the series.

For any side of the yield surface the total derivative of the yield function may be written as

$$\frac{\partial F^i}{\partial \sigma_{ij}} d\sigma_{ij} + \frac{\partial F^i}{\partial h} dh = 0 \quad (12)$$

Combining Eqns. 11 and 12 as illustrated in Ref. [7] leads to a relationship between stress and strain in the form

$$\delta\sigma_{ij} = (\underline{D}_e - \underline{D}_e \left\{ \frac{\partial F^i}{\partial \sigma_{ij}} \right\} \underline{M}^{-1} \left\{ \frac{\partial F^i}{\partial \sigma_{ij}} \right\}^T \underline{D}_e) \delta\varepsilon_{ij} \quad (13)$$

This defines the elasto-plastic matrix as

$$\underline{D}_{ep} = \underline{D}_e - \underline{D}_e \left\{ \frac{\partial F^i}{\partial \sigma_{ij}} \right\} \underline{M}^{-1} \left\{ \frac{\partial F^i}{\partial \sigma_{ij}} \right\}^T \underline{D}_e \quad (14)$$

in which

$$\underline{M} = A^i + \left\{ \frac{\partial F^i}{\partial \sigma_{ij}} \right\}^T \underline{D}_e \left\{ \frac{\partial F^i}{\partial \sigma_{ij}} \right\} \quad (15)$$

and

$$A^i = - \frac{\partial F^i}{\partial \eta} \sigma_{ij} \frac{\partial F^i}{\partial \sigma_{ij}} \quad (16)$$

At corners of the yield surface, where functions F^i and F^j intersect, the flow rule is written as

$$\delta \epsilon_{ij}^p = \lambda^i \frac{\partial F^i}{\partial \sigma_{ij}} + \lambda^j \frac{\partial F^j}{\partial \sigma_{ij}} \quad (17)$$

and thus Eqn. 11 is modified to

$$\delta \epsilon_{ij} = \underline{D}_e^{-1} \delta \sigma_{ij} + \lambda^i \frac{\partial F^i}{\partial \sigma_{ij}} + \lambda^j \frac{\partial F^j}{\partial \sigma_{ij}} \quad (18)$$

The elasto-plastic matrix for a corner is then found by combining Eqn. 18 with the derivatives of each of the functions F^i and F^j to give

$$\underline{D}_{ep} = \underline{D}_e - \underline{D}_e \begin{bmatrix} \frac{\partial F^i}{\partial \sigma_{ij}} & \frac{\partial F^j}{\partial \sigma_{ij}} \end{bmatrix} \underline{M}^{-1} \begin{bmatrix} \frac{\partial F^i}{\partial \sigma_{ij}} & \frac{\partial F^j}{\partial \sigma_{ij}} \end{bmatrix}^T \underline{D}_e \quad (19)$$

where

$$\underline{M} = \underline{A} + \begin{bmatrix} \frac{\partial F^i}{\partial \sigma_{ij}} & \frac{\partial F^j}{\partial \sigma_{ij}} \end{bmatrix} \underline{D}_e \begin{bmatrix} \frac{\partial F^i}{\partial \sigma_{ij}} & \frac{\partial F^j}{\partial \sigma_{ij}} \end{bmatrix} \quad (20)$$

and

$$\underline{A} = \begin{bmatrix} A^i & A^i \\ A^j & A^j \end{bmatrix} \quad (21)$$

NUMERICAL EXAMPLE

The plane stress problem indicated in Fig. 3 was selected to illustrate the use of the linearized yield surface for tension-weak material because for this problem the material yields on Side Three of the yield surface (see Fig. 2b), where the two principal stresses are of opposite signs. This problem is similar to the rigid punch problem but here a uniform pressure is applied in lieu of imposed displacements.

Due to symmetry about a vertical plane, it was necessary to model only half of the figure shown. One hundred and eighteen (118) constant strain elements were used in the finite element mesh.

Two cases were solved. In the first case a tension-weak material was assumed to have a compressive yield stress, σ_{yc} , of 4 Ksi and a tensile yield stress, σ_{yt} , of 0.4 Ksi. Thus $\alpha = \sigma_{yc}/\sigma_{yt} = 10.0$. In the second case the compressive and tensile yield stresses were equal at 4 Ksi ($\alpha = 1.0$). In both cases elastic-perfectly plastic behavior was assumed. Also constant for both cases were Young's Modulus, E , at 3.6×10^3 Ksi and Poisson's Ratio, ν , at 0.2. The representative uniaxial stress-strain curves for both cases are shown in Fig. 4.

The progression of the yielded region with increasing load for the first case ($\alpha = 10.$, tension-weak material) is shown in Fig. 5 and that for the second case ($\alpha = 1.0$) is shown in Fig. 6 for comparison. In these figures the load level is indicated in non-dimensional form. Values given are for $p/2\sigma_{yc}$ where p is the applied pressure.

It is immediately obvious that the forms of the yielded regions and the load levels required to cause a significant yield area are vastly different for the two cases. The first case is somewhat analogous to the conical failure surface of a concrete cylinder subjected to compressive force in that a wedge of material directly under the applied force retains its integrity while it becomes separated from the rest of the body by a region of yielded material. The second case is more like a metallic specimen, incurring a plastic region directly under the applied load. These analogies tend to support the rationality of the results.

CONCLUSION

The research reported here has shown that the linearized yield surface for tension-weak material can be made compatible with a non-linear finite element analysis method. And it is seen from the example problems that the use of the linearized yield surface gives results that model real behavior to some degree and in the least represents an improvement over linear elastic analysis for tension-weak materials. The authors found the analyses relatively easy to perform: numerical stability was not a problem and convergence in the iterative process was rapid. It is expected that research now in progress will numerically substantiate that in certain cases the linearized yield surface represents an approximation within the bounds of accuracy employed in engineering practice.

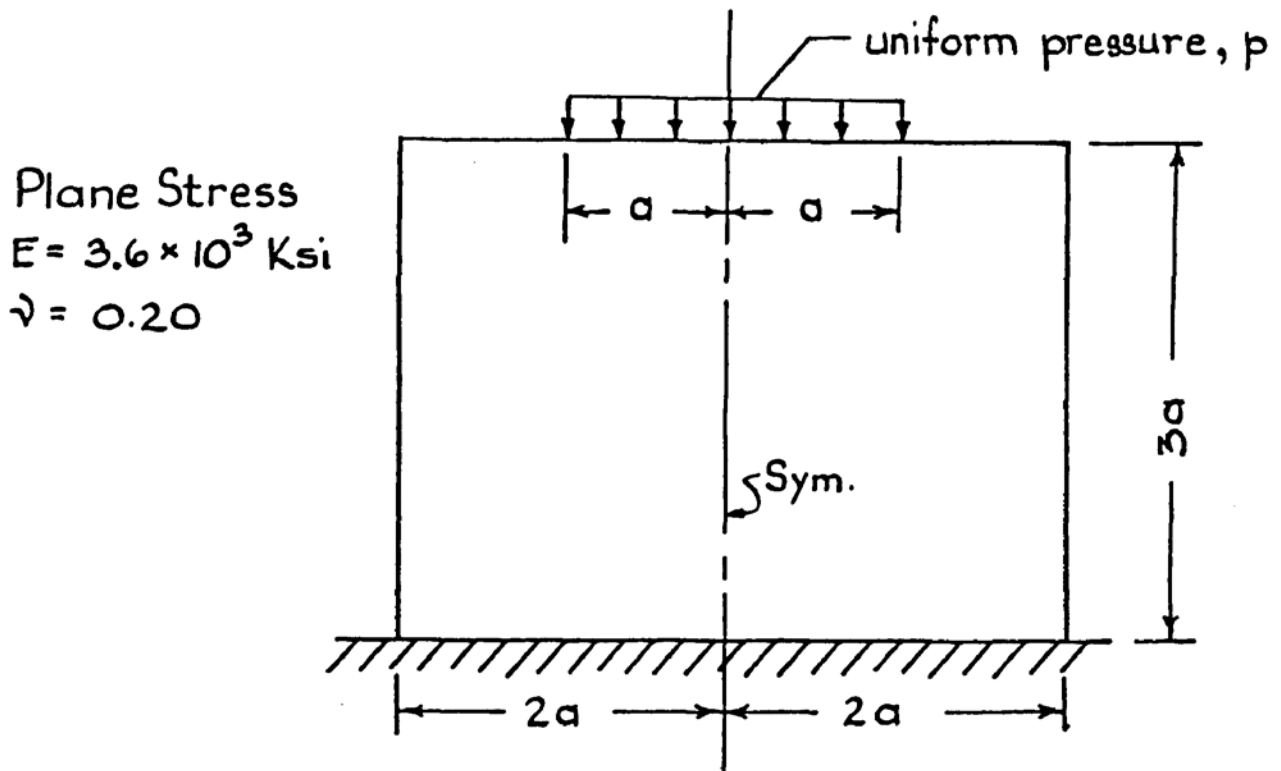


Figure 3. Problem For Numerical Example

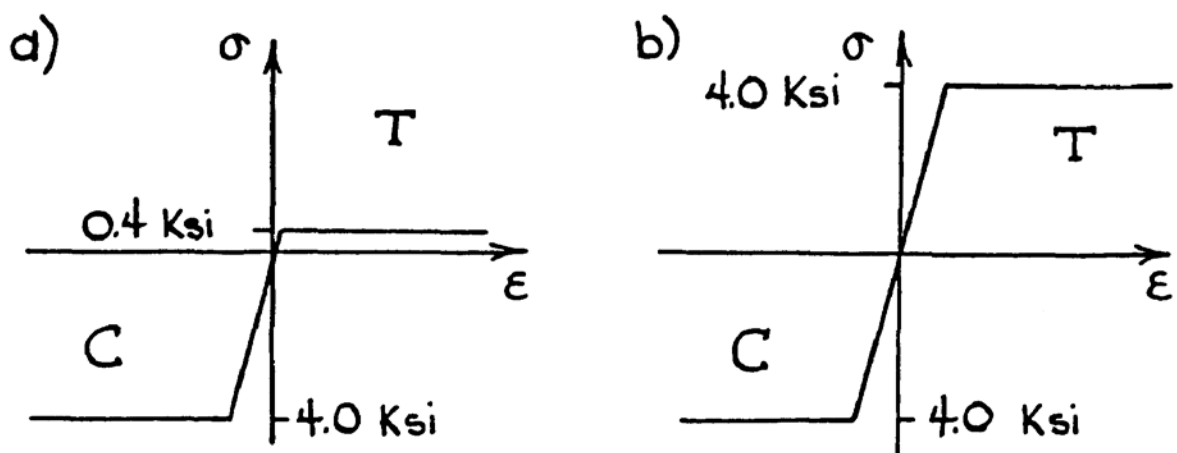


Figure 4. Uniaxial Stress-Strain Curves For Example Problem

a) for $\alpha = 10.0$; b) for $\alpha = 1.0$.

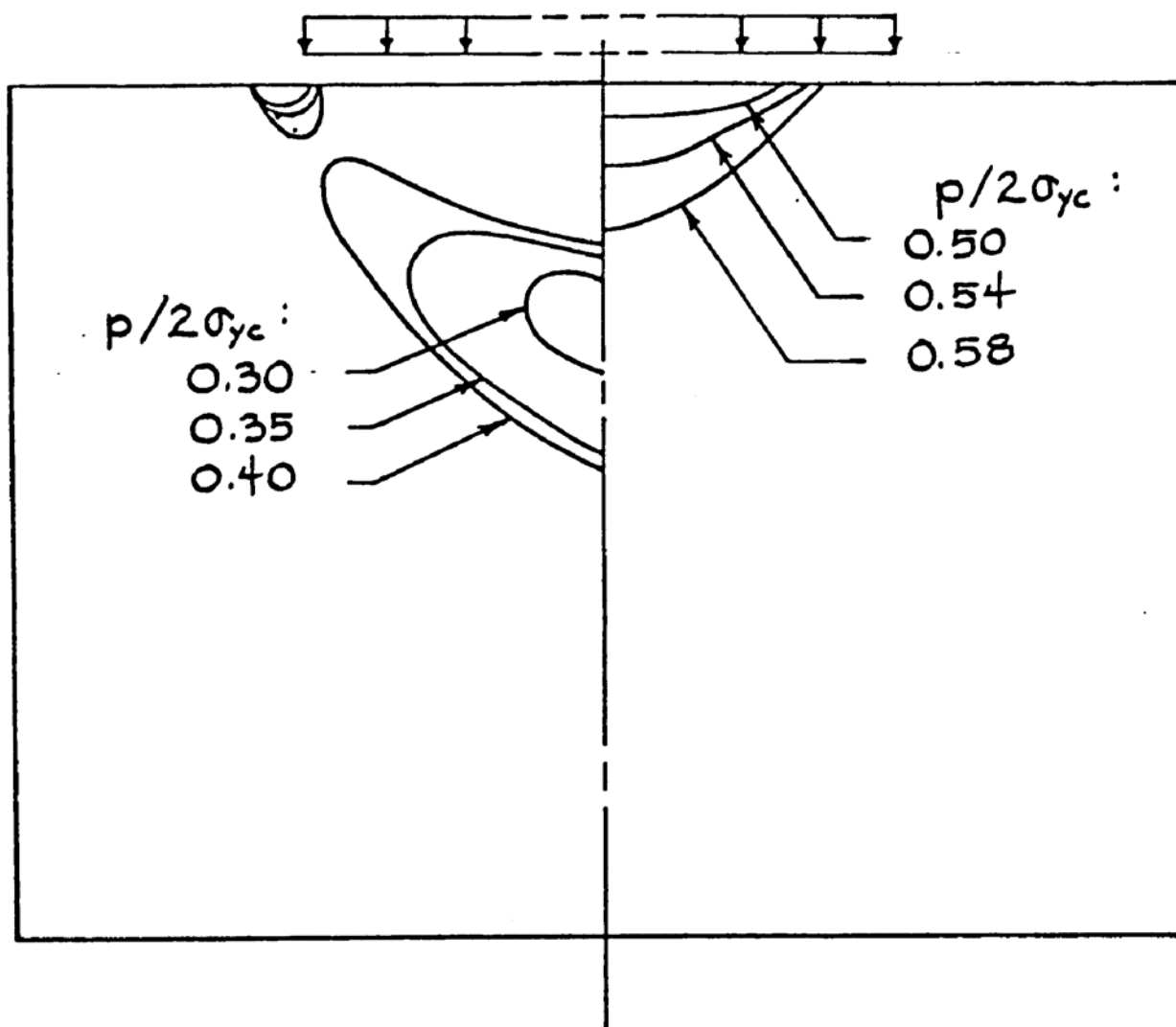


Figure 5. Progression Of The
Yielded Region For
 $\alpha = 10.0$

Figure 6. Progression Of The
Yielded Region For
 $\alpha = 1.0$

REFERENCES

1. Gerstle, K. H., "Simple Formulation of Biaxial Concrete Behavior," ACI Journal, Jan. 1981, pp. 62-68.
2. Chen, A. C. T. and Chen, W. F., "Constitutive Relations for Concrete," J. of the Engng. Mechs. Div., ASCE, EM4, August, 1975, pp. 465-481.
3. Buyukozturk, O., "Nonlinear Analysis of Reinforced Concrete Structures," Computers and Structures, Vol. 7, 1977, pp. 149-156.
4. Darwin, D. and Pecknold, D.A., "Nonlinear Biaxial Stress-Strain Law for Concrete," J. of the Engng. Mechs. Div., ASCE, EM2, April, 1977.
5. Zienkiewicz, O. C., Valliappan, S. and King, I. P., "Elasto-Plastic Solutions of Engineering Problems: 'Initial Stress' Finite Element Approach," Int. J. for Num. Methods in Engng., Vol. 1, 1970, pp. 75-100.
6. Weisgerber, F. E. and Anand, S. C., "Interpolative vs. Iterative Solution Schemes for Tresca Yield Condition in Elastic-Plastic Finite Element Analysis," Int. J. for Num. Methods in Engng., Vol. 12, 1978, pp. 765-777.
7. Anand, S.C. and Weisgerber, F.E., "Inelastic Finite Element Analysis Using Tresca Yield Condition," J. of the Engng. Mechs. Div., ASCE, EMI, February 1977, pp. 1-16.